J. Breath Res. **1** (2007) 026003 (9pp) doi:10.1088/1752-7155/1/2/026003

Non-invasive and isotope-selective laser-induced fluorescence spectroscopy of nitric oxide in exhaled air

Christoph Mitscherling[1], Jörg Lauenstein[1], Christof Maul[1], Alexei A Veselov[2], Oleg S Vasyutinskii[2] and Karl-Heinz Gericke[1]

[1] Department of Physical and Theoretical Chemistry, University of Braunschweig, Hans-Sommer-Str. 10, 38106 Braunschweig, Germany
[2] Ioffe Institute Saint Petersburg, 26 Polytekhnicheskaya, St Petersburg 194021, Russian Federation

E-mail: c.mitscherling@tu-bs.de

Received 1 May 2007
Accepted for publication 12 October 2007
Published 8 November 2007
Online at stacks.iop.org/JBR/1/026003

Abstract
The detection of nitric oxide (NO) is of considerable medical interest. NO is involved in a multitude of mammal physiological processes, and various non-invasive concentration determination methods for NO have been developed during the last few years. Regarding time resolved metabolism behavior the quantitative determination of the $^{15}N^{16}O$-isotopologue in combination with ^{15}N-labeled drugs and amino acids is a central interest of current medical research. We apply laser-induced fluorescence (LIF) spectroscopy for isotope-selective detection of NO in various biological environments with a theoretical detection limit below 0.1 parts per trillion (ppt). Electronic excitation of the AX-transition in the UV provides fluorescence around 247 nm from $A^2\Sigma^+(v' = 0) \longrightarrow X^2\Pi_\Omega(v'' \geqslant 2)$. For an online measurement of human exhaled air, a respiratory mask has been constructed and integrated into our system. This paper gives an overview of the applied LIF device for non-invasive detection of NO originated from exhaled human air. The main advantages of this device compared to established methods are as follows: high sensitivity for NO concentrations in the ppt region, a high time resolution of 20 ms and isotopic selectivity to distinguish between ^{14}NO and ^{15}NO. Visualizations of single-exhalation profiles and long-time online measurements including the determination of absolute NO concentrations are presented and the influence of quenching gases present during the experiment is discussed. To our knowledge, we present for the first time time-resolved ^{15}NO online profiles of exhaled human air.

1. Introduction

Nitric oxide (NO) is responsible for a multitude of processes in the atmosphere and in the physiology of mammals, plants and bacteria. The global output of NO_x is in the range of 38 Mt/a, where the main contributor is anthropogenic fuel combustion with a percentage of about 55% [1]. Besides this global relevance in ozone depletion of the stratosphere and ozone accumulation in the lower troposphere, it was found in the 1980s that NO in low concentrations is important for messaging and regulation processes inside the human body. NO also plays a central role as a signal molecule in the growth and differentiation processes of plants [2–4].

In the human body, different types of NO-synthase (NOS) catalyze a 5-electron oxidation of a terminal nitrogen atom of the amino acid L-arginine to produce NO and citrulline [2, 5]. This NO is involved in blood pressure regulation of the cardiovascular system, immune defense and neurotransmission. For their work on the role of NO in the human body and, especially, the discovery that NO is identical to the endothelium derived relaxing factor (EDRF) [6] which seemed to be responsible for blood pressure regulation before 1986, F Furchott [7], L J Ignarro and F Murad received in 1998 the Nobel Prize for Physiology or Medicine. Since then the research on NO has been more and more intensified,

yielding numerous annual publications, specialized journals and meetings.

The production of NO via NOS is highly complex and until now not completely understood but has been found in all vertebrate groups. At the moment, three main isoforms of NOS are known to be responsible for diverse tasks. Endothelial NOS (eNOS) regulates vascular tone, blood pressure and inhibition of platelet aggregation, neuronal NOS (nNOS) is present in the neuronal network of the brain producing NO for neurotransmission (both Ca^+-dependent) and inducible NOS (iNOS) expressed in macrophages which participate in immune defense (Ca^+-independent). The latter is mainly responsible for NO in the human respiratory tracts and therefore represents an important marker for the diagnosis and supervision of inflammatory diseases [5].

For detailed information about disease-evoked NO enhancement and its time resolved metabolism behavior, a multitude of non-invasive and invasive methods concerning the determination of absolute NO concentrations has been developed during the last few years and tried to be standardized [8, 9]. Especially breath analysis as an instrument for non-invasive analysis with spectroscopic methods [10–20] is well established and of great interest [21, 22]. The observation of exhaled air is, for example, nowadays a standard procedure to assist asthma patients [23–26]. Commercial devices (e.g. NIOX®) achieve detection limits in the lower parts per billion (ppb) ranges with averaging times of a few seconds. Besides the main compounds of exhaled air such as N_2, O_2, CO_2 and H_2O, volatile organic compounds (VOCs) have been known for a long time as indicators of special diseases and are therefore important keys for non-invasive diagnostics [27].

We apply laser-induced fluorescence (LIF) spectroscopy for real time observation of NO originating from biological samples. A main advantage of LIF is the extremely high sensitivity with a theoretical detection limit in the sub-parts per trillion (ppt) range combined with isotopic selectivity. This method is able to distinguish between the main isotopologues $^{14}N^{16}O$ with an abundance of 99.393% due to the natural isotopic distribution, $^{15}N^{16}O$ (0.369%) and $^{14}N^{18}O$ (0.199%) [28]. The integration of a breath mask allows isotope selective online observations with a time resolution of 20 ms. Both high-resolution single-exhalation profiles and long-time monitoring of exhaled air from patients allow tracer experiments with doted drugs or amino acids such as ^{15}N doted L-arginine [29] to be performed.

2. Theory

2.1. Spectroscopy of NO

LIF spectroscopy is the most sensitive method for the determination of NO concentrations with a theoretical detection limit below 0.1 ppt [30, 31]. The introduced device combines both extreme sensitivity and isotopic selectivity in static and online experiments for non-invasive analysis of NO produced in biological systems.

LIF spectroscopy is applied by electronic excitation of the $3s\sigma$-Rydberg transition $A^2\Sigma^+(v' = 0) \longleftarrow X^2\Pi_\Omega(v'' = 0)$ around 226.5 nm and time-delayed observation of the $A^2\Sigma^+(v' = 0) \longrightarrow X^2\Pi_\Omega(v'' \geqslant 2)$ fluorescence around 247.4 nm. All possible transitions are well known and tabulated [31, 32]; the natural lifetime of the excited state is 205 ± 7 ns for $A^2\Sigma^+$, $v' = 0$ [33]. The vibrational ground level $v'' = 0$ is sufficiently populated at room temperature whereas $v'' \geqslant 2$ is unpopulated for relaxation. Fluorescence to $v'' < 2$ and excitation light is blocked by an interference filter to make sure that no excitation light is detected. The $\gamma(0)$-band in the near ultraviolet (NUV) is relatively weak compared to $\gamma(\leqslant 1)$ but convenient for the wavelength of the applied laser system. Other transitions such as BX and DX also occur at lower wavelengths and have much lower natural lifetimes. The excitation energy of our laser system is high enough to work at the saturation limit. Accordingly, the energy fluctuation of the laser has a negligible effect on the observed fluorescence.

Since the concentration of ^{15}NO, due to natural isotopic distribution, is about 270 times less than that of ^{14}NO, the detection of this isotopologue has to take place in a region with no ^{14}NO adsorption around 225.965 nm. During the experiment a constant transition is used $P_1(10.5;7.5)$ for ^{14}NO and $P_1(8.5;9.5)$ for ^{15}NO [31]. Neglecting effects such as self-quenching of NO, which is acceptable for concentrations of 500 ppb and below, the observed total fluorescence is proportional to the concentration of NO in the sample. In combination with the standard addition method (SAM) [34] or calibration curves it is possible to determine absolute concentrations with high accuracy.

2.2. Quenching effects and optimal cell pressure

Generally, in fluorescence measurements quenching is a phenomenon deserving special attention. Considering concentrations in the lower ppb region and below makes the effect of self-quenching of NO negligible. But especially with regard to breath measurements water, CO_2 and O_2 contained in the sample reduce the observable fluorescence because of the natural lifetime reduction of the excited state due to non-radiative deactivation. This effect is pressure dependent and has been investigated intensively to determine the optimal pressure for fluorescence measurements. Furthermore, factors have been experimentally determined and calculated to take quenching effects into account when applying calibration curves for concentration determination. When determining low NO concentrations with the SAM, quenching effects have no impact on the calculated concentration. To reduce the contribution of water to the overall fluorescence decrease due to quenching a Nafion dryer tube (Perma Pure MD-070-24S-4) can be applied to reduce the humidity ratio.

We assume an instantaneous excitation of the NO molecules in the sample. The number $N_1(t)$ of excited molecules at time t divided by the number of excited molecules at the time of laser excitation $N_1(t_0)$ is proportional to the fluorescence intensity $I(t)$ and describes an exponential decrease

$$\frac{N_1(t)}{N_1(t_0)} = \frac{I(t)}{I_0} = \exp[-k_F \cdot t] = \exp\left[\frac{-t}{\tau_{\text{nat}}}\right] \qquad (1)$$

with k_F being the reciprocal natural lifetime τ_{nat} of the excited state. So the total fluorescence intensity I_T is given by

$$I_T = \int I(t)\,\mathrm{d}t = \int_0^\infty I_0 \cdot \exp\left[\frac{-t}{\tau_{\text{nat}}}\right]\mathrm{d}t = I_0 \cdot \tau_{\text{nat}} \qquad (2)$$

and for the real boxcar delay-time $t_D > 0$ for fluorescence observation in reference to the trigger signal

$$I_T \geqslant I_{\text{obs}} = I_0 \cdot \int_{t_D}^{t_G} \exp\left[\frac{-t}{\tau_{\text{nat}}}\right]\mathrm{d}t. \qquad (3)$$

t_D is the temporal delay of the boxcar from a trigger signal correlating with the excitation of NO and the fluorescence signal afterwards. $t_D > 0$ prevents the boxcar from detecting excitation light. The time t_G is the gate duration for boxcar integration. The fluorescence intensity is proportional to the number of excited NO molecules and hence proportional to the total number of NO molecules N_0 in the sample. The correlation $I_T \propto N_1(t_0) \propto N_0 \propto p(\text{NO}) \propto p$ leads to

$$I_T = A \cdot p, \qquad (4)$$

with A being a constant, p the overall pressure and p(NO) the partial pressure of NO. In the presence of quenching gases, the natural lifetime τ_{nat} in (1) needs to be replaced by the experimentally observed lifetime τ_{obs},

$$\tau_{\text{obs}} = \frac{1}{k_F + \sum k_{Q,i} \cdot x_i \cdot p}, \qquad (5)$$

with $k_{Q,i}$ being the quenching constant of compound i and $x_i \cdot p$ the partial pressure of compound i. Considering that $k_Q = \sum k_{Q,i} \cdot x_i \cdot p$ is the overall quenching constant, insertion in (2) and integration from t_A to ∞ yields (6) for the total observed fluorescence intensity I_{obs},

$$I_{\text{obs}} = \frac{A_q \cdot p \cdot k_F}{k_F + k_Q \cdot p} \cdot \exp[-t_D(k_F + k_Q \cdot p)], \qquad (6)$$

with A_q being a constant and t_D the delay time for fluorescence observation of the boxcar in reference to the trigger signal. When $t_D = 0$, for very low pressures (6) is a straight line with slope A_q. For higher pressures the curve reaches a maximum and falls again to zero for very large pressures, considering $t_D \geqslant 0$. Pressure-dependent measurements of the fluorescence intensity have been made and compared with the theoretical values with the use of known quenching constants of the main air components [31]. Accordingly, the optimal pressure for air and exhaled air measurements concerning the fluorescence concentration is about 12 mbar in the cell.

2.3. Considerations of cross-sensitivities and errors during the measurement

As mentioned before, the concentration of ^{15}NO in the observed samples is about 270 times less than the concentration of ^{14}NO due to the natural isotopic distribution. Hence, ^{14}NO peaks in the recorded spectra are considerably more intense than the ^{15}NO counterpart. For isotope-selective detection possible cross-sensitivities should be excluded.

Line broadening that occurs consists of effects from (natural) lifetime broadening, collisional broadening, Doppler broadening and the line broadening of the applied dye laser. The laser manufacturer specifies the full width at half maximum to be 6×10^9 s^{-1}. Considering a Gaussian behavior of all the terms mentioned above, the overall broadening is about 6.7×10^9 s^{-1}, showing that line broadening of the dye laser is the critical factor. The theoretical overall broadening should be below 30 GHz to resolve ^{15}NO beside ^{14}NO. Experimental data fitted to a normal probability curve showed laser-line width between 17 and 20 GHz due to adjustment of the dye laser. Hence, the contribution of ^{14}NO to the total measured signal during the ^{15}NO measurement due to overlap of transitions is negligibly small.

Furthermore, the chemical composition of the observed sample needs some special attention. Exhaled air is supposed to contain about 1200 compounds and trace gases [35]. In general, the concentration of most compounds is negligibly small. Nevertheless some considerations should be mentioned.

- Compounds react with NO, reducing the observable NO concentration: since the concentrations of both NO and trace gases are very low kinetic considerations have been made for the most important reactions, for example with ozone and oxygen. Ozone concentrations about 100 ppb lead to half-life times for NO of 4 h. The trimolecular reaction with oxygen leads to half-life times of several years. So the reduction of the NO concentration by reactions with other trace gases is not a decisive factor compared to the duration of performed experiments.
- Trace gases raising the NO concentration by photochemical generation of NO: generation from the elements is negligible since temperatures over 3000 K have to be applied. Photodissociation of NO_2 occurs when applying wavelengths up to 398 nm. We calculated an increase of NO concentration per pulse of 0.01%, showing that photodissociation does not increase the NO concentration significantly during the experiment. In addition, the applied flux during online measurements avoids accumulation. Photodissociation of other trace gases is even more improbable.
- Absorption of the excitation wavelength is not important for the experiment. All main trace gases have small cross-sections or very low concentrations and therefore no considerable effect. For NO_2 the attenuation is about a factor of 2×10^{-12}.
- Fluorescence is absorbed, reducing the detectable NO concentration: as in the previous point, this effect is negligible. The attenuation factor for NO_2 is about 1.1×10^{-8}.
- Other trace gases emitting the same fluorescence wavelength: measured NO spectra from exhaled air are in excellent agreement with the calculated ones (Pgopher 5.2 [36]). Comparison of exhaled air NO spectra with spectra from pure NO shows identical intensity proportions, which proves that NO is the only detected molecule during online experiments.

2.4. Calibration and the standard addition method

LIF is no absolute method, so calibration of the system is essential. Besides the application of common calibration curves the SAM has been applied. The main disadvantage of

calibration curves is the problem of comparing measurements of different composition because of varying overall quenching constants. In principle, it is possible to take equation (6) into account to calculate the intensity change due to quenching effects.

The application of the SAM is more convenient because the unknown sample is turned into a standard itself. In the first step the intensity of the unknown sample is measured and then different amounts of known NO concentrations are added by the mass-flux system described in section 3.5. Plotting the respective fluorescence intensities versus NO concentration leads to the unknown NO concentration value of the sample. For a mathematical description, see [34].

The basis for this method is the proportionality between fluorescence signal intensity and NO concentration. This is true for low NO concentrations below 500 ppb with a negligibly small effect of self-quenching (nevertheless this can be again taken into account by application of equation (6)). By addition of small amounts of NO compared to the applied flux of the unknown sample the overall sample composition relative to the quenching-gas composition remains almost the same during the whole SAM procedure and changes in quenching are negligibly small. Usual dilutions are in the range of 1–0.1%. The added samples are different mass fluxes of a 2.5 ppm NO mixture (certified 2.5 vol. ppm NO in N_2, Westfalen AG, uncertainty 5%). The mass flux controllers have an uncertainty of 1% of the maximum range. So, the SAM is adequate for a dynamical determination of absolute NO concentrations originated from different biological environments. In addition, it offers high precision due to linear regression and is independent from external parameters such as photomultiplier voltage or boxcar sensitivity. The main disadvantage of the SAM is the high expenditure of time and the fact that many samples are needed which should be of constant concentration during the whole procedure. This can be avoided by using breath-sample bags for the SAM and comparison with the averaged intensity of single-exhalation profiles from online experiments. With the help of this method it is possible to assign absolute concentrations in online experiments.

For ^{15}NO concentration determinations it is supposed that the applied certified 2.5 ppm NO mixture consists of the NO isotopologues due to the natural isotopic distribution. Comparison of SAM results from ^{14}NO and ^{15}NO in exhaled human air (14 ± 2 ppb and 47 ± 5 ppt, respectively) leads to a factor of 298 ± 53 between the two signals that is in the range of the theoretical value.

3. Experimental setup

The main components of the applied device for LIF spectroscopy of ^{14}NO and ^{15}NO are a laser system consisting of a XeCl excimer laser and a dye laser, a measuring cell and a reference cell, detection optics, signal processing and a mass-flux system. Furthermore, a breath mask for online human exhaled air measurements has been integrated.

3.1. XeCl excimer and dye laser system

The laser radiation at wavelengths around 226 nm is generated by a XeCl excimer pumped dye laser which is frequency-doubled with a β-barium borate crystal (BBO) (figure 1). The XeCl excimer laser (Lambda Physik LPX 600) is triggered internally or externally by a pulse generator (Quantum Composers 9514). The laser-pulse generating arc discharge is variable between 16.1 kV and 24.0 kV with a maximum repetition rate of 50 Hz. If not otherwise mentioned, we applied 18 kV discharge voltage at 5 Hz to obtain pump pulse energies between 130 mJ and 140 mJ. The incidental pump wavelength of 308 nm has temporal full width at half maximum of about 50 ns with a spectral full width at half maximum of about 0.5 nm.

The dye laser (Lambda Physik FL 2002) offers a broadband fluorescence between 440 nm and 484 nm with an emission maximum at 456 nm applying Coumarin 47 (1.59 g l^{-1} for the oscillator/preamplifier and 0.53 g l^{-1} for the main amplifier) in MeOH. For wavelength separation a grating ($K = 600$ grooves mm^{-1}, 2.7 micron blaze, zerodur substrate) is used in the third order, generating a beam with a spectral broadening of 0.6 cm^{-1} and pulse durations of 30 ns. Recirculation of the MeOH solution prevents the dye from photobleaching.

The frequency doubling device for the second harmonic generation (SHG) contains the BBO crystal and a stepper motor for computer-aided tracking of the BBO while changing the wavelength. This system has to be calibrated in the applied wavelength region before scanning. During the calibration procedure in a desired wavelength range the BBO crystal is aligned to maximum energy output on five different positions for automatic tracking during a scan. The frequency doubled pulse energies are between 250 μJ and 800 μJ. A Pellin-Broca prism is used to separate the dye incidental wavelength from the frequency doubled wavelength. Two prisms situated on the beam path direct the beam to the measuring cell.

3.2. Measuring cell

The beam enters the measuring cell (MC) through a fused quartz window with Brewster-angle ($\Theta_B = 57.2^\circ$ for air/fused quartz) to prevent reflection loss. A blackened Woods–Horn perpendicular to the incoming beam prevents interference from back reflections of the windows. Each cell contains on input and output sides two pinholes of 4 mm diameter to minimize scattered light. The cubic cell of 10 cm side length contains boreholes of 8 cm diameter on each side. A second MC is used as a reference cell to monitor the laser performance during long-time measurements. When the system is not operated both cells are constantly kept under a vacuum.

3.3. Detection optics

Inside the MC detection optics perpendicular to the incoming excitation beam focuses the fluorescence on a photomultiplier tube (PMT) (see figure 2). A f/1 lens collects and collimates the fluorescence. The collected light passes through a fused

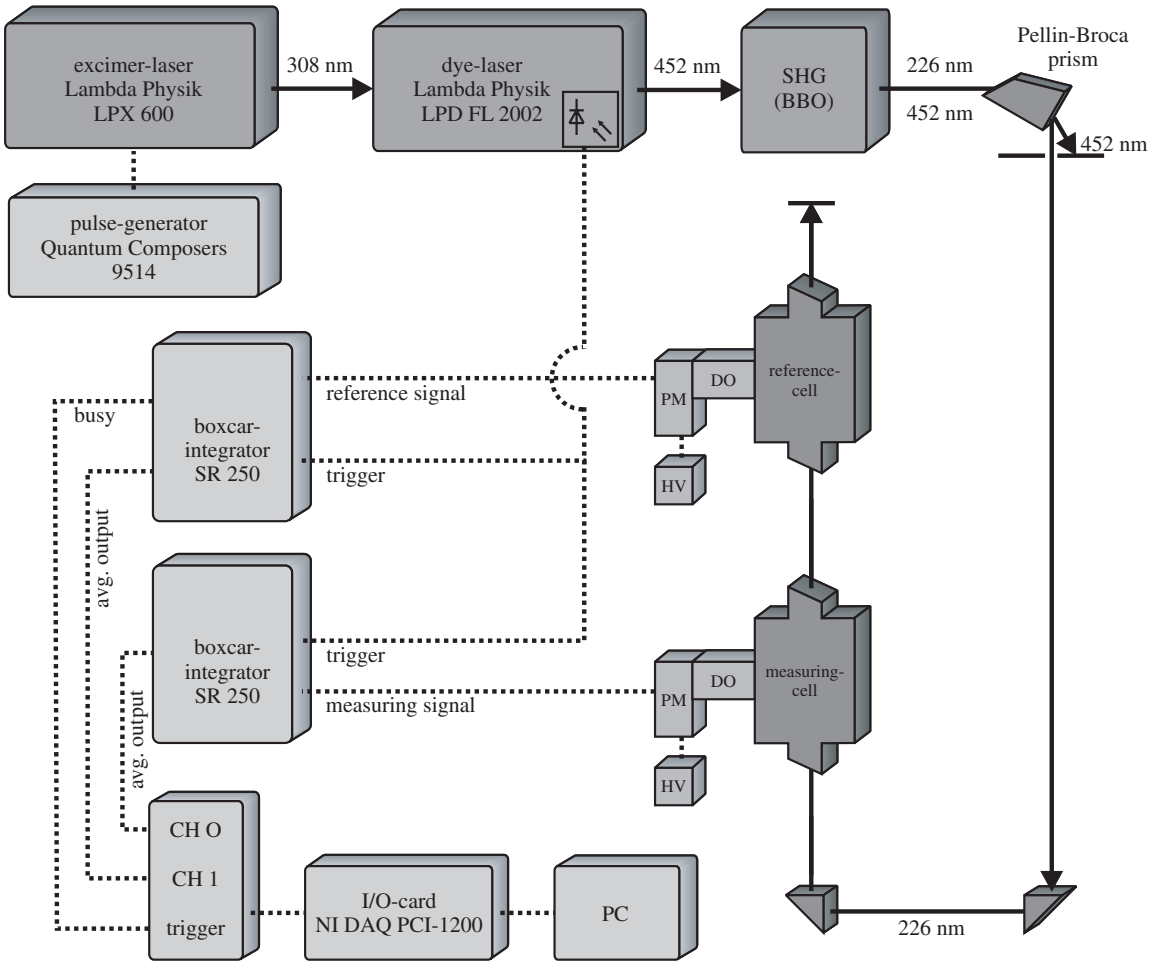

Figure 1. A schematic overview of the laser system and signal processing. SHG: second harmonic generation; DO: detection optics; PM: photomultiplier; HV: high voltage power supply.

quartz window that seals the cell from the environment and is then filtered by an interference filter (Andover Corporation 248FS10-50) with a transmission for fluorescence (247.4 nm) and excitation light (226 nm) of 12% and 0.3%, respectively. A pinhole in front of the photomultiplier prevents diffuse incoming radiation from being detected. The side-on photomultiplier (Hamamatsu R3788) consists of nine dynodes which can be operated at a maximum voltage of 1500 V. The photomultiplier is mounted inside a copper tube and fixed to the detection optics. The signal output is connected to a boxcar integrator (Stanford Research Systems SR 250).

3.4. Signal processing

The PM signals are integrated with a boxcar integrator (BI) and recorded by a PC. The BI is able to accept voltages between −2 V and +2 V. The incoming voltage can be integrated by applying variable integration times (t_G) from 1 ns to 16.3 μs. The time delay t_D between 1 ns and 100 ms is stepless tunable. For most experiments we apply a delay time of $t_D = 20$ ns to avoid interference from excitation light and integration times of $t_G = 300$ ns with a boxcar input resistance of 50 Ω. Furthermore, averaging is possible to improve the signal-to-noise (SN) ratio. The output signal in the range of −10 V to +10 V is led into an analog/digital transducer and then to a multi-I-O-PC plug-in card. A LabVIEW program (National Instruments Corporation) is used for visualizing and saving the data in ASCII format.

The BI is triggered for synchronization by a photodiode mounted inside the dye laser detecting scattered light.

3.5. Mass-flux system

The mass-flux system is in general designed to meet a large variety of specific requirements. It is able to analyze both static and online concentrations of NO with high accuracy. The cubic cell is equipped with DN16 and DN40 flanges connecting the different devices described in this section (figure 3).

Since the pressure for optimal signal intensity of exhaled air is around 12 mbar the pressure inside the measuring chamber is controlled dynamically by a pressure controller device (MKS Instruments 250E) while different mass fluxes are applied. The pressure is monitored by a capacity pressure gauge head (MKS Instruments Baratron 221 AHS-D-100, 0.1–100 mbar) in the measuring cell and controlled by an electromagnetic valve (MKS Instruments 248A). The electromagnetic valve and an optional bypass for handling bigger mass flows are connected to a piston pump (Pfeiffer Vakuum XtraDry 150-2).

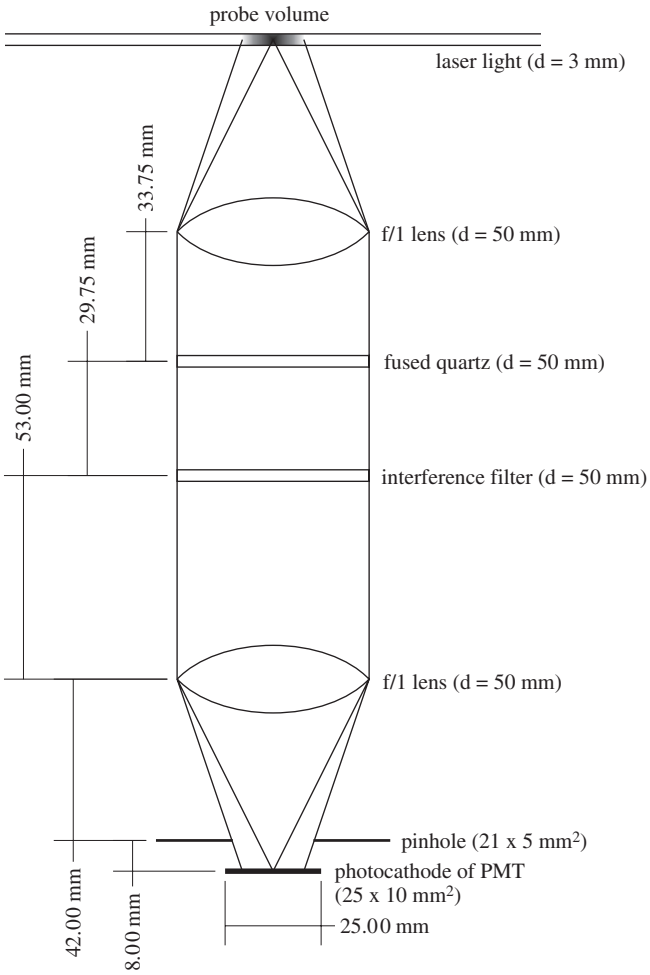

Figure 2. A schematic overview of the detection optics.

The variable mass flow to the measuring cell is controlled by a mass flow control unit (MKS Instruments PR4000) operating two mass flow controllers (MKS Instruments 1179A). The sample mass-flux controller (MFC) provides volumetric flow rates of 20–2000 sccm min^{-1}; the calibration gas MFC which is used to apply the SAM provides a flow rate between 0.2 and 10 sccm min^{-1}.

Figure 4. Picture of the breath mask for online exhaled air measurements.

Gas samples can be observed directly or can be prepared before observation. All polyvinyl fluoride (PVF) lines are equipped with Swagelok connectors so that the sample inlet can easily be changed for the purpose of a measurement. For example, a breath mask in combination with a Nafion tube for gas drying can be applied.

3.6. The breath mask

For the time-resolved investigation of exhaled human breath a breath mask has been constructed and integrated in our device (figures 4 and 5). While the test person inhales, ambient air flows into the mask through valve A. When exhaling, A is closed and the exhaled air flows through valve B and the mass flow controller into the measuring cell. Inhaling again, valve B is closed and valve C opens to rinse the cell with pure nitrogen. This device allows observation of single-exhalation profiles with a maximum resolution of 20 ms over several hours. The test person is able to breathe under normal conditions effortlessly.

4. Results and discussion

Spectra can be recorded of both ^{14}NO and ^{15}NO in the region of interest. The recorded spectra are in excellent agreement

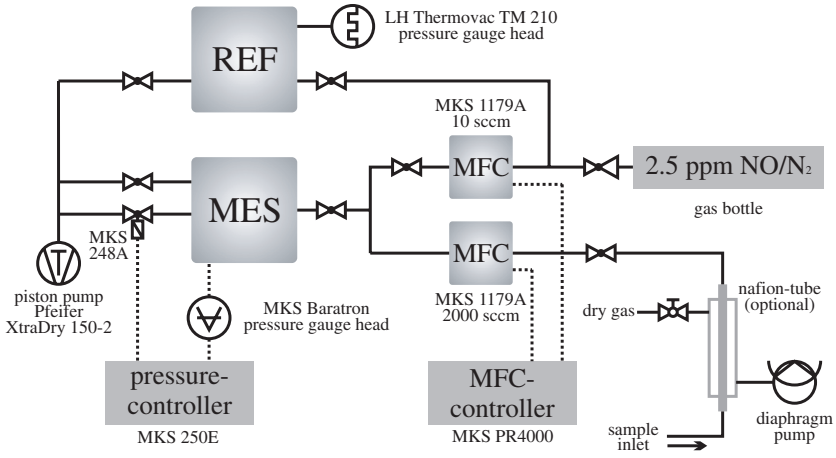

Figure 3. A schematic overview of the applied mass-flux system. MES: measuring cell; REF: reference cell; MFC: mass-flux controller.

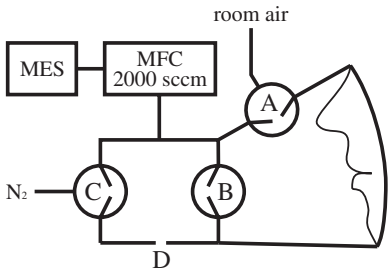

Figure 5. Schematic overview of the breath mask for online exhaled air measurements. MFC: mass-flux controller; MES: measuring cell; A, B, C: valves; D: overpressure hole.

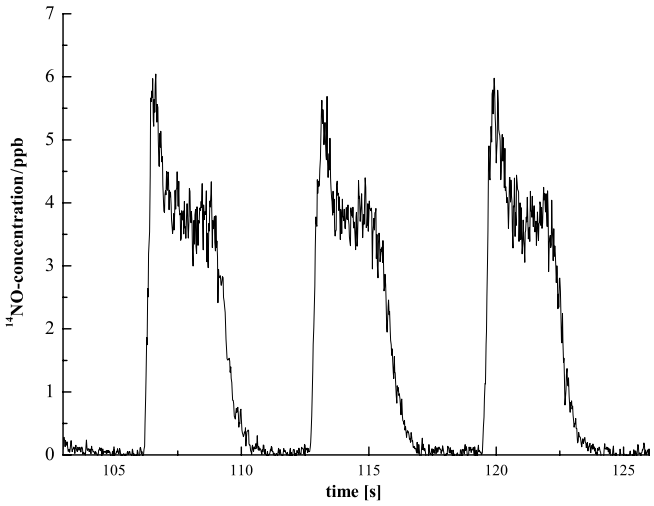

Figure 6. Small section of a long-time online exhaled air measurement showing single-exhalation profiles of ^{14}NO.

with the calculated ones. The region between 225.955 nm and 225.985 nm is suitable for ^{15}NO measurements because of the absence of strong transitions from ^{14}NO. For the ^{14}NO detection we use the $P_1(10.5;7.5)$ transition of the γ-band at 225.953 nm which is piloted by the dye laser before the measurement. During the whole experiment the excitation wavelength remains the same. The reference cell is filled with a standard NO mixture (2.5 ppm NO in N_2) at 12 mbar (fixed) whose signal is observed for the total measuring time. By this reference system the laser power is monitored in order to recognize and record effects such as energy fluctuations due to temperature changes in the BBO crystal.

Operating the breath mask with flows of about 1200 sccm min^{-1} we are able to monitor both single-exhalation profiles and long-term exhalation profiles 'online' with a resolution of 20 ms over several hours (figures 6 and 7). The shape of those exhalation profiles is as expected. Each profile begins with an initial peak representing air from the dead volume of the respiratory tract of about 300 ml. The following plateau is air from the lung. The respiration time differs from person to person as well as the amount of exhaled NO. For lung NO concentrations we observed values between 4 ppb and 50 ppb from six healthy test persons. One asthma patient showed lung NO concentrations about 120 ppb due to inflammatory stress. All presented measurements are profiles from breathing

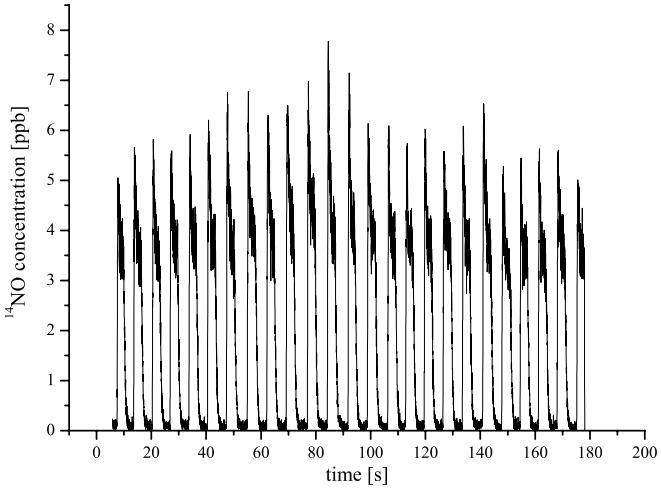

Figure 7. Section from long-time online exhaled air measurement showing single-exhalation profiles of ^{14}NO.

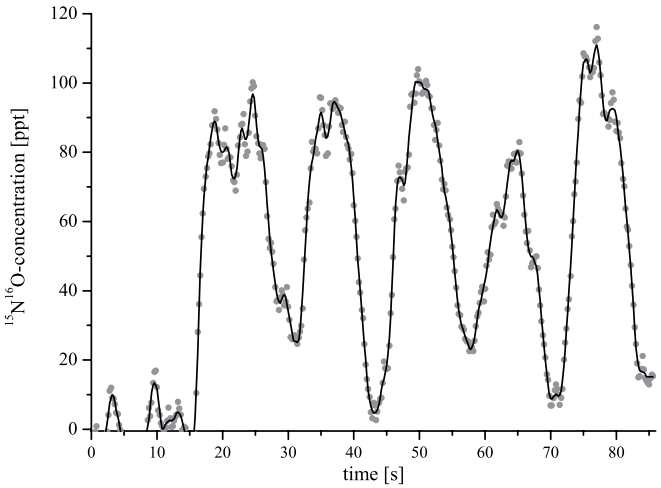

Figure 8. Small section of a long-time online exhaled air measurement showing single-exhalation profiles of ^{15}NO. The first 15 s is just pure N_2. The straight line is an average over 20 points.

with the mouth. Exhalation by the nose yields higher NO concentrations. The higher noise of the plateau is within a normal range in comparison with the baseline with an even better signal-to-noise ratio. The non-zero concentration of the baseline is an effect of PM noise and small amounts of NO in the applied N_2 during rinse cycles. The determination of the absolute NO concentration has been done by using the well established SAM, as described in section 2.4. Lauenstein *et al* [31] demonstrated the validity of this method in measuring an increase of exhaled ^{15}NO after oral intake of ^{15}N-labeled L-arginine. Whereas these experiments proved the accuracy of our device, those online exhaled air measurements have been applied, to our knowledge, for the first time for observation of time resolved ^{15}NO profiles (figure 8). The concentration of those online measurements is in the lower ppt region and opens up new vistas on the time resolved metabolism behavior of doted amino acids and drugs producing ^{15}NO. According to section 2.4, the averaged NO concentrations of single-exhalation profiles have been measured with the

SAM to be 80.25 ± 6.19 ppt. This value is within the range of physiological expected values due to the natural isotopic distribution and known ^{14}NO concentrations from online measurements. The practical detection limit of this method has been experimentally measured to be 3.70 ± 0.33 ppt corresponding to a signal-to-noise ratio of 2.

5. Conclusions and perspectives

It has been shown that LIF spectroscopy as a platform for time-resolved and isotope-selective detection and absolute determination of NO concentration is an accurate and fast method for a diversity of scientific problems. The device introduced is able to collect precise information about NO concentrations of biologically relevant samples. A non-invasive online observation of both ^{14}NO and ^{15}NO originated from exhaled human air with a maximum time resolution of 20 ms down to concentrations in the lower ppt region has been demonstrated. Hence, this device is more sensitive than current commercially used devices with an increased time resolution and isotopic selectivity.

For further improvement we want to apply a longpass filter having higher transmissions around 247 nm. Additional usage of the fluorescence signal from the $v'' = 1$ transition will increase the overall fluorescence intensity. Shorter excitation pulse durations should improve boxcar gating and thus increase the applicable pressure, yielding more fluorescence. Furthermore, higher excitation energies combined with a telescope in the excitation beam optics tend to result in the utilization of a bigger excitation volume in the measuring cell. Combination of these upgrades makes a detection of NO in the sub-ppt region possible as well as the online detection of exhaled $^{14}N^{18}O$. For further observation of time resolved NO production inside the human body, we applied LIF for determination of NO output due to cutaneous respiration to support breath analysis and thus introduce an additional method for non-invasive analysis.

References

[1] Delmas R, Serca D and Jambert C 1997 Global inventory of NO_x sources *Nutr. Cycling Agroecosys.* **48** 51–60

[2] Lamattina L, García-Mata C, Graziano M and Pagnussat G 2003 Nitric oxide: the versatility of an extensive signal molecule *Ann. Rev. Plant Biol.* **54** 109–36

[3] Planchet E and Kaiser W M 2006 Nitric oxide production in plants *Plant Signal. Behav.* **1** 46–51

[4] del Rio L A, Corpas F J and Barroso J B 2004 Nitric oxide and nitric oxide synthase activity in plants *Phytochemistry* **65** 783–92

[5] Groves J T and Wang C C-Y 2000 Nitric oxide synthase: models and mechanism *Curr. Opin. Chem. Biol.* **4** 687–95

[6] Ignarro L J, Buga G M, Wood K S, Byrns R E and Chaudhuri G 1987 Endothelium-derived relaxing factor produced and released from artery and vein is nitric oxide *Proc. Natl Acad. Sci. USA* **84** 9265–9

[7] Furchgott R F 1999 Endothelium-derived relaxing factor: Discovery, early studies, and identification as nitric oxide (Nobel lecture) *Angew. Chem. Int. Edn* **38** 1870–80

[8] Kharitonov S, Alving K and Barnes P J 1997 ERS task force report; exhaled and nasal nitric oxide measurements: recommendations *Eur. Respir. J.* **10** 1683–93

[9] American Thoracic Society Documents 2005 ATS/ERS recommendations for standardized procedures for the online and offline measurement of exhaled lower respiratory nitric oxide and nasal niric oxide *Am. J. Respir. Crit. Care Med.* **171** 912–30

[10] Volz A and Drummond J W 1984 Messung von Stickoxiden im ppt-Bereich durch Chemilumineszenz mit O_3^* *Fresenius Z. Anal. Chem.* **317** 355–8

[11] Hanna S F, Barron-Jimenez R, Anderson T N, Lucht R P, Caton J A and Walther T 2002 Diode-laser-based ultraviolet absorption sensor for nitric oxide *Appl. Phys.* B **75** 113–7

[12] Roller C, Namjou K, Jeffers J D, Camp M, Mock A, McCann P J and Grego J 2002 Nitric oxide breath testing by tunable-diode laser absorption spectroscopy: application in monitoring respiratory inflammation *Appl. Opt.* **41** 6018–29

[13] Bakhirkin Y A, Kosterev A A, Roller C, Curl R F and Tittel F K 2004 Mid-infrared quantum cascade laser based off-axis integrated cavity output spectroscopy for biogenic nitric oxide detection *Appl. Opt.* **43** 2257–66

[14] Halmer D, von Basum G, Horstjann M, Hering P and Mürtz M 2005 Time resolved simultaneous detection of ^{14}NO and ^{15}NO via mid-infrared cavity leak-out spectroscopy *Isot. Environ. Health Stud.* **41** 303–11

[15] Kosterev A A, Malinovsky A L, Tittel F K, Gmachl C, Capasso F, Sivco D L, Baillargeon J N, Hutchinson A L and Cho A Y 2001 Cavity ringdown spectroscopic detection of nitric oxide with a continious-wave quantum-cascade laser *Appl. Opt.* **40** 5522–9

[16] Mürtz P, Menzel L, Bloch W, Hess A, Michel O and Urban W 1999 LMR spectroscopy: a new sensitive method for on-line recording of nitric oxide in breath *J. Appl. Physiol.* **86** 1075–80

[17] Sich I and Russow R 1999 ^{15}N analysis of nitric oxide and nitrous oxide by cryotrap enrichment using a gas chromatograph quadrupole mass spectrometer and its application to ^{15}N-tracer investigations of NO/N_2O formation in soil *Rapid Commun. Mass Spectrom.* **13** 1325–8

[18] Lee S-H, Hirokawa J, Kajii Y and Akimoto H 1997 New method for measuring low NO concentrations using laser induced two photon ionization *Rev. Sci. Instrum.* **68** 2891–7

[19] Simeonsson J B, Lemire G W and Sausa R C 1994 Laser-induced photofragmentation/photoionization spectrometry: A method for detecting ambient oxides of nitrogen *Anal. Chem.* **66** 2272–8

[20] Reeves M, Musculus M and Farell P 1998 Confocal, two-photon laser-induced fluorescence technique for the detection of nitric oxide *Appl. Opt.* **37** 6627–35

[21] Amann A, Schmid A, Scholl-Bürgi S, Telser S and Hinterhuber H 2005 Breath analysis for medical diagnosis and therapeutic monitoring *Spectrosc. Eur.* **17** 18–20

[22] Himashree G, Dass D, Banerjee P K and Selvamurthy W 2003 Nitric oxide and the respiratory system *Curr. Sci.* **85** 607–14

[23] Smith A D, Cowan J O, Brasset K P, Herbison G P and Taylor D R 2005 Use of exhaled nitric oxide measurements to guide treatment in chronic asthma *N. Engl. J. Med.* **352** 2163–73

[24] Kharitonov S A and Barnes P J 2000 Clinical aspects of exhaled nitric oxide *Eur. Respir. J.* **16** 781–92

[25] Guo F H, Comhair S A A, Zheng S, Dweik R A, Eissa N T, Thomassen M J, Calhoun W and Erzurum S C 2000 Molecular mechanisms of increased nitric oxide (NO) in asthma: evidence for transcriptional and post-translational regulation of NO synthesis *J. Immunol.* **164** 5970–80

[26] Delclaux C, Mahut B, Zerah-Lancner F, Delacourt C, Laoud S, Cherqui D, Duvoux C and Harf A 2002 Increased

nitric oxide output from alveolar origin during liver cirrhosis versus bronchial source during asthma *Am. J. Respir. Crit. Care Med.* **165** 332–7

[27] Manoli A 1983 The diagnostic potential of breath analysis *Clin. Chem.* **29** 5–15

[28] http://physics.nist.gov/PhysRefData/Elements/index.html May 2007

[29] Lauenstein J and Gericke K-H 2005 Isotope selective detection of nitric oxide in human exhalation *Breath Analysis for Clinical Diagnosis and Therapeutic Monitoring* ed A Amann and D Smith (Singapore: World Scientific) chapter B, pp 161–9

[30] Winefordner J D and Rutledge M 1985 Comparison of calculated detection limits in molecular absorption, molecular luminescence, Raman, molecular ionization and photothermal spectrometry *Appl. Spectrosc.* **39** 377–91

[31] Lauenstein J 2006 Isotopenselektiver Nachweis von biologisch freigesetztem Stickstoffmonoxid *Dissertation* TU-Braunschweig

[32] Luque J and Crosley D R 1999 Transition propabilities and electronic transition moments of the $A^2\Sigma^+ - X^2\Pi$ and $D^2\Sigma^+ - X^2\Pi$ systems of nitric oxide *J. Chem. Phys.* **111** 7405–15

[33] Luque J and Crosley D R 2000 Collisional energy transfer of NO $D^2\Sigma^+(v' = 0)$ and $A^2\Sigma^+(v' = 4)$ by O_2, N_2, Ar and NO *J. Phys. Chem.* A **104** 2567–72

[34] Ingle J D Jr and Crouch S R 1988 *Spectrochemical Analysis* (Englewood Cliffs, NJ: Prentice-Hall)

[35] Philips M 1997 Method for the collection and assay of volatile organic compounds in breath *Anal. Biochem.* **247** 272–8

[36] Western C M 2007 Pgopher, a program for simulating rotational structure, University of Bristol, version 5.2 (http://pgopher.chm.bris.ac.uk/